Comparative Analysis of Quadratic Buck-Boost Converters: Topology, Electric Stress, Reliability.

SVK Naresh and Sankar Peddapati
Department of Electrical Engineering
National Institute of Technology Andhra Pradesh, India-534101.
svknaresh.sclr@nitandhra.ac.in and sankarp@nitandhra.ac.in

IECON 2021 - 47th Annual Conference of the IEEE Industrial Electronics Society | 978-1-6654-3554-3/21/$31.00 ©2021 IEEE | DOI: 10.1109/IECON48115.2021.9589610

***Abstract*— In this article, a comprehensive review of quadratic buck-boost converters has been presented. Due to the wide conversion ratio, these converters are suitable for intermittent renewable sources like PV systems for power generation. This article aims to compare the quadratic buck-boost converters in terms of structural difference, the total electric stress experienced by power semiconductor devices, efficiency, and few other features. Further, the reliability of these converters is estimated with the help of the Markov chain model, and converters are compared with a mean time to failure period. Finally, the merits and demerits of each converter are explained.**

Keywords*— *dc-dc converter, electric stress, quadratic buck-boost voltage gain, steady-state analysis, reliability.

I. Introduction

The carbon emissions and climatic changes motivated the human community to work towards renewable energy generation. Which is eco-friendly and has shown great promise for future electricity needs with the help of a power electronic interface. The typical renewable energy generation and integration to the grid are shown in Fig. 1. From the figure, a dc-dc converter is used to extract the maximum available power from the source with the help of an MPPT controller. Further, an inverter is used for the integration to the grid for domestic applications.

A dc-dc converter with a wide conversion ratio is required as the renewable sources are intermittent due to their dependency on environmental conditions. The conventional buck-boost, Cuk, SEPIC, and ZETA converters have a wide conversion ratio with step-up/down capabilities [1]. Among the converters mentioned above, the Cuk converter has an advantage of continuous input and continuous output current, which makes it superior to others for renewable energy applications. Even though all the buck-boost type converters have a high voltage gain theoretically, it is very limited in practical applications due to the parasitic nature of circuit components. In order to improve the voltage gain, transformer-based converters have been used by adjusting the turn ratio. However, the size and cost of the transformer is the drawback of these converters [2]. Alternatively, the voltage multiplier cell (VMC) based converters have evolved for higher voltage gain. These are formed with a switched capacitor or switched inductor cells and are applied to conventional dc-dc converters to achieve improved voltage gain. These converters are cost-effective and have a simple structure, yet, they suffer from the instantaneous overcurrent phenomenon of a capacitor and less efficiency [3-7]. Further, the coupled-inductor-based converters are reported for the improved voltage gain [8-10]. But these converters have the limitation of leakage inductance, which causes the unwanted voltage surges at the power semiconductor devices during the switching transition, and also have limited switching frequency. The most popular and feasible solution to improve

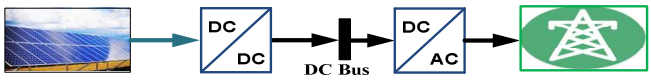

Fig. 1. Grid integration of renewable energy sources.

the voltage gain is cascading the conventional converters. They are also called quadratic converters due to the quadratic nature of voltage gain with respect to duty ratio. The cascaded converters are introduced with the help of basic switching cells [11]. Then, quadratic buck converters with a high step-down ratio are presented along with their single switch topologies [12]. But these converters are not suitable for renewable energy generation due to the lack of high step-up gain. However, the research on quadratic buck converters is limited. On the other hand, quadratic boost converters are heavily reported in terms of different configurations [13-16], semi-quadratic topologies [17-18], and control techniques [19]. The quadratic boost converters find many applications like renewable power generation and electric vehicles due to their high voltage gain capability. Alternatively, the quadratic buck-boost converters provide a wide conversion ratio essential for intermittent renewable power generation. The conventional quadratic buck-boost converter (CQBBC) and its derived single switch topology are introduced [12]. But it has a drawback of discontinuous input and discontinuous output current. Afterward, many quadratic buck-boost topologies were reported by modifying the CQBBC for added advantages like continuous input and continuous output current [20-23]. A converter is proposed to achieve the benefits mentioned above by cascading a boost, buck-boost, and buck converters and is modified to a single switch topology [24]. Recently, three enhanced gain buck-boost converters are proposed a quadratic conversation ratio, and these converters exhibit good dynamic response [25].

The power electronic converters play a crucial role in the renewable integration to the grid as shown in Fig. 1. Unfortunately, power electronic devices and capacitors are the most sensitive and prone to failure due to electric stress [26-27]. So, reliability studies of power electronic converters are necessary to estimate the lifetime of the system. The evaluation metrics are failure rate (λ), reliability function with respect to operating hours (R(t)), and mean time to failure MTTF (in hours). The mathematical representation of these metrics is given below.

$$\begin{cases} \mathrm{R(t)} = \mathrm{e}^{-\int_0^{\infty} \lambda(\mathrm{t})\,\mathrm{dt}} = \mathrm{e}^{-\lambda \mathrm{t}} \\ \mathrm{MTTF} = \int_0^{\infty} \mathrm{R(t)}\,\mathrm{dt} = \frac{1}{\lambda} \end{cases} \tag{1}$$

In this article, an attempt is made to compare all these quadratic buck-boost converters in terms of various essential performance indices like electric stress, efficiency, and reliability. This article's organization is as follows; the description of quadratic buck-boost converters is given in section II. The comparative analysis in section III and reliability evaluation is followed by section IV, and finally, the conclusion and remarks are given in section V.

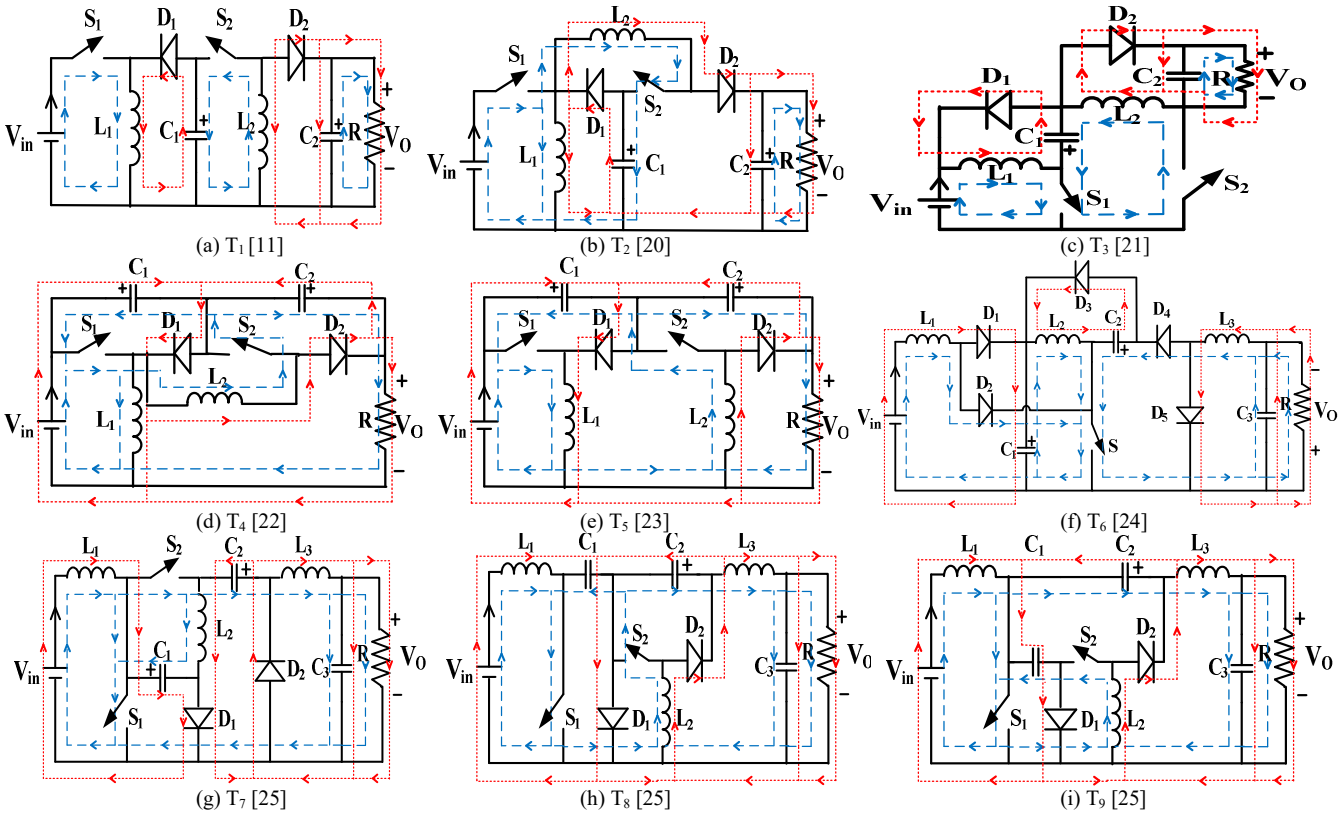

Fig. 2. Quadratic buck-boost converters.

II. Quadratic Buck-Boost Converters

In this section, the details about constructional features and the operation of quadratic buck-boost converters are discussed. There are nine topologies designated T_1 to T_9. The details of these topologies are as follows.

Topology-1 (T_1): This is formed by the cascaded connection of two buck-boost converters, as shown in Fig. 2(a). This converter is treated as a conventional quadratic buck-boost converter (CQBBC). When the two active switches are ON, inductors will magnetize, and capacitors will be discharged. When the two active switches are turned OFF, the inductors will be demagnetized, and capacitors will get charged. The power flow of the converter during ON state and OFF state are represented with red and blue color lines, respectively. Despite the wide conversation ratio, the CQBBC has a disadvantage of discontinuous input and output current.

Topology-2 (T_2): This converter is proposed by Shan Miao et al. for quadratic buck-boost gain [20] modifying the CQBBC as shown in Fig. 2(b). Here, the location of the second inductor has changed. It is also a fourth-order circuit with two synchronously operated active switches. The operating modes of ON and OFF state are depicted in Fig. 2(b). When switches are turned ON, the inductors draw the energy from the source and capacitor and release it to the capacitor and load during turn OFF state. However, this converter also does not have the continuous input and continuous output current feature.

Topology-3 (T_3): This converter is proposed by Ali et al. for the wide conversion ratio [21] and is shown in Fig. 2(c) along with operating modes. This converter is a fourth-order circuit with two synchronously operated switches. When the switches are turned ON, diodes will be reverse biased, resulting in inductors getting magnetized and capacitors discharged. In the case of OFF state, the diodes will be forward biased. The inductors and capacitors will get demagnetized and charged, respectively. Unfortunately, this converter has limitations like discontinuous input, and there is no common ground between input and output terminals.

Topology-4 (T_4): This converter [22] is proposed by Julio et al. and is shown in Fig. 2 (d). This converter is formed by modifying the CQBCC to achieve the continuous input and continuous output and applied for proton exchange membrane fuel cell (PEMFC) conversion systems. Because of the mentioned modifications, this topology requires high voltage output capacitors. Here, the location of the two capacitors and the second inductor has changed.

Topology-5 (T_5): This is converter [23] is formed by modification CQBBC and is shown in Fig. 2 (e). The modification is that the location of capacitors has changed to achieve the continuous input and continuous output current. However, the major demerit is that it requires high voltage capacitors compared to CQBBC.

Topology-6 (T_6): A single switch converter is proposed for quadratic buck-boost gain with continuous input and continuous output capabilities [24] and is shown in Fig. 2(f). This converter is formed by cascading the boost, buck-boost, and buck converters; and then reduced to a single switch topology. Due to the cascading connection of three basic dc-dc converters, the usage of power devices (1 switch and five diodes) and passive elements (3 inductors and three capacitors) is high. In addition, it has a drawback of negative output polarity.

Topology-7 (T_7), Topology-8 (T_8), and Topology-9 (T_9): These three converters are the family of enhanced gain buck-boost converters [25] proposed by M Veerachary et al., and

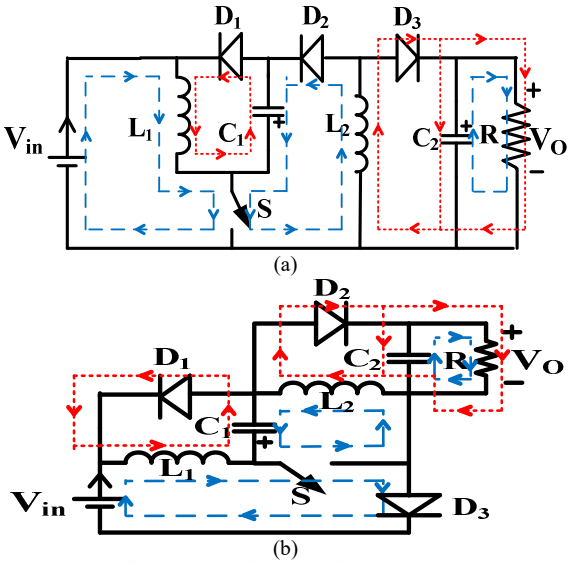

Fig. 3. Single switch topologies of (a) T_1 and (b) T_3.

The circuit diagram of T_7, T_8, and T_9 is shown in Fig. 2(g), Fig. 2(h), and Fig. 2(i), respectively. These converters consist of two synchronously operated active switches, two diodes, three inductors, and three capacitors. Among three EGBBC converters, T_7 is a minimum phase system, and T_8, T_9 are non-minimum phase systems. These three converters produce the quadratic buck-boost gain along with added features like continuous input and output current and positive polarity.

Among the above nine topologies, T_1 and T_3 have the possibility of deriving a single switch topology using the Graft scheme [28]. When there is a common node between two synchronously operating active switches, it can be reduced to a single switch. The single switch topology of T1 is reported in [12] and is shown in Fig. 3(a). The single switch topology of T3 is derived in this work by using a Graft scheme and is shown in Fig. 3(b). The operating modes of these single-single switch topologies are also demonstrated in Fig. 3. These converters give the same steady-state results as two switch topologies.

III. Comparative Analysis

In this section, the comparative analysis of all the quadratic buck-boost converters is presented. The comparison is made in terms of the number of components used, the voltage and electric stress of power devices, total voltage stress, total current stress, the switching device power rating (SDP), efficiency, and few other features like an order of the system, continuous input current, continuous output current, the output polarity, availability of common ground. The comprehensive comparison of quadratic buck-boost converters (T_1 to T_7) is tabulated in Table I. Here, only topology T_7 is considered for the comparison, as T_8 and T_9 exhibit similar performance.

From Table I, the conventional quadratic buck-boost converter its modified converters are fourth-order circuits, using a smaller number of components. In contrast, the converter [24] uses a higher number of power semiconductors and passive components compared to other converters. The order of the system is higher for the converters in [24] and [26]. It leads to difficulty in the controller design for the system. In the case of fourth-order circuits, the switch S_2 in the converter [21] experience higher voltage stress than other converters. The voltage and current stress experienced by

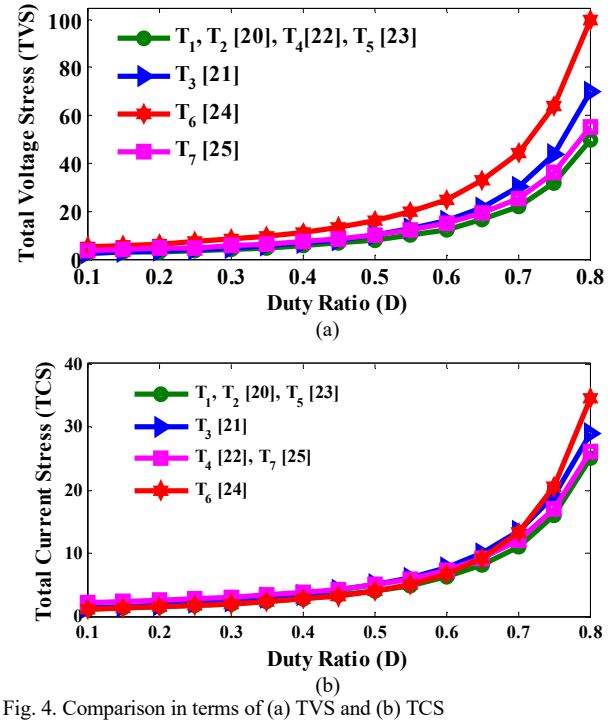

Fig. 4. Comparison in terms of (a) TVS and (b) TCS

power semiconductor devices can be represented with total voltage stress (TVS) and total current stress (TCS). The comparison of quadratic buck-boost converters compared in terms of TVS and TCS and is shown in Fig. 4. From the figure, it is clear that topology T_6 [24] experience the highest TVS and TCS compared to other converters. It is pretty evident that T_6 uses a higher number of power devices as compared to other converters. In contrast, CQBBC and its modified converters are shown better performance in terms of TVS and TCS.

In addition, the quadratic buck-boost converters are compared with the cost function of power converters, i.e., the switching device power rating [18]. The cost of the power converters depends on the number of power devices and their electric stress. The SDP of a converter is calculated as follows.

$$SDP = \sum_{i=1}^{n} V_{Si} * I_{Si} \quad (2)$$

Where n is the number of power devices in the converter, and V_S and I_S are the voltage and current experienced by the power switch. Since the gain of all converters is the same, the SDP of quadratic converters can be represented with respect to duty ratio and is shown in Fig. 5. It is evident that the SDP of topology T_6 [24] is higher than other converters because of the number of power devices and the high electric stress. The computer-based MATLAB simulations are carried out to estimate the efficiency of the quadratic buck-boost converters. The circuit parameters used in the simulation are given in Table II. Table I shows that the efficiency of T_2 is higher, and T_6 has lower efficiency than the remaining converters.

Further, the topologies T_4, T_5, T_6, T_7 have the continuous input current and continuous output current with the common ground between input and output terminals, which are essential for renewable power extraction. However, the converter the topology T_7 [25] is the best among all quadratic converters because it is a minimum phase system. Whereas remaining topologies are non-minimum phase systems. So, the controller design and the dynamic behavior of the topology, T_7 is superior to the rest of the coverters.

TABLE I. COMPARATIVE ANALYSIS OF QUADRATIC BUCK-BOOST CONVERTERS

Topology		T_1	T_2[20]	T_3[21]	T_4[22]	T_5[23]	T_6[24]	T_7[25]
No. of	Switches	2	2	2	2	2	1	2
	Diodes	2	2	2	2	2	5	2
	Inductors	2	2	2	2	2	3	3
	Capacitors	2	2	2	2	2	3	3
Total		8	8	8	8	8	12	10
Order of the converter		4	4	4	4	4	6	6
Voltage Gain ($\lvert V_O/V_{in}\rvert$)		$\left(\frac{D}{1-D}\right)^2$	$\left(\frac{D}{1-D}\right)^2$	$\left(\frac{D}{1-D}\right)^2$	$\left(\frac{D}{1-D}\right)^2$	$\left(\frac{D}{1-D}\right)^2$	$\left(\frac{D}{1-D}\right)^2$	$\left(\frac{D}{1-D}\right)^2$
Voltage Stress on Switch (V_S/V_{in})	S_1	$\frac{1}{1-D}$	$\frac{1}{1-D}$	$\frac{1}{1-D}$	$\frac{1}{1-D}$	$\frac{1}{1-D}$	$\frac{1}{(1-D)^2}$	$\frac{1}{1-D}$
	S_2	$\frac{D}{(1-D)^2}$	$\frac{D}{(1-D)^2}$	$\frac{2D}{(1-D)^2}$	$\frac{D}{(1-D)^2}$	$\frac{D}{(1-D)^2}$		$\frac{1}{(1-D)^2}$
Voltage Stress on Diode (V_D/V_{in})	D_1	$\frac{1}{1-D}$	$\frac{1}{1-D}$	$\frac{1}{1-D}$	$\frac{1}{1-D}$	$\frac{1}{1-D}$	D_1, D_4: $\frac{1}{1-D}$; D_2, D_5: $\frac{D}{(1-D)^2}$	D_1: $\frac{1}{1-D}$
	D_2	$\frac{D}{(1-D)^2}$	$\frac{D}{(1-D)^2}$	$\frac{D}{(1-D)^2}$	$\frac{D}{(1-D)^2}$	$\frac{D}{(1-D)^2}$	D_3: $\frac{1}{(1-D)^2}$	D_2: $\frac{D}{(1-D)^2}$
Total Voltage Stress		$\frac{2}{(1-D)^2}$	$\frac{2}{(1-D)^2}$	$\frac{2+D}{(1-D)^2}$	$\frac{2}{(1-D)^2}$	$\frac{2}{(1-D)^2}$	$\frac{4}{(1-D)^2}$	$\frac{3-D}{(1-D)^2}$
Current Stress on Switch (i_S/i_O)	S_1	$\left(\frac{D}{1-D}\right)^2$	$\left(\frac{D}{1-D}\right)^2$	$\frac{D}{(1-D)^2}$	$\left(\frac{D}{1-D}\right)^2$	$\left(\frac{D}{1-D}\right)^2$	$\frac{D^3-D^2+D}{(1-D)^2}$	$\left(\frac{D}{1-D}\right)^2$
	S_2	$\frac{D}{1-D}$	$\frac{D}{1-D}$	$\frac{D}{1-D}$	$\frac{1}{1-D}$	$\frac{D}{1-D}$		$\frac{1}{1-D}$
Current Stress on Diode (i_D/i_O)	D_1	$\frac{D}{1-D}$	$\frac{D}{1-D}$	$\frac{D}{1-D}$	$\frac{D}{1-D}$	$\frac{D}{1-D}$	D_1: $\frac{D^2}{1-D}$; D_2: $\frac{D^3}{(1-D)^2}$	D_1: $\frac{D}{1-D}$
	D2	1	1	1	1	1	D_3, D_4, D_5: D, $1-D$	D_2: 1
Total Current Stress		$\frac{1}{(1-D)^2}$	$\frac{1}{(1-D)^2}$	$\frac{1+D-D^2}{(1-D)^2}$	$\frac{2-2D+D^2}{(1-D)^2}$	$\frac{1}{(1-D)^2}$	$\frac{1+2D^3-D^2}{(1-D)^2}$	$\frac{2-2D+D^2}{(1-D)^2}$
Continuous input		×	×	×	√	√	√	√
Continuous output		×	×	√	√	√	√	√
Positive output		√	√	√	√	√	×	√
Common ground		√	√	×	√	√	√	√
Efficiency (%) at 100 W		85.42	87.97	84.14	86.47	83.52	80.62	85.5

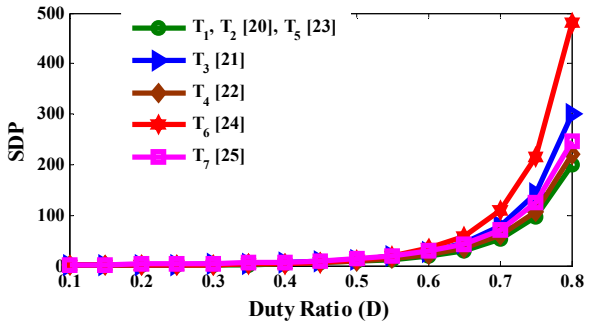

Fig. 5. SDP comparison of all the converters.

TABLE II. CIRCUIT PARAMETERS

Parameter	Rating
Input voltage	12 V
Output power	100 W
Load Resistance	120 Ω
Inductance	L_1=L_2= L_3= 2 mH
Capacitance	C_1=C_2=C_3= 220 μF
Switching Frequency	20 kHz

IV. Reliability Evaluation

The reliability of power converters depends significantly on the life time of the power switch and electrolytic capacitors as they are the most sensitive components to fail. The failure rate of these components decides the lifetime period of the whole system. The failure rate indicates the proneness to failure, and it follows the bathtub curve with respect to time. Here, the constant failure rate method is adopted to evaluate the reliability of quadratic buck-boost converters. However, it has limitations like not considering wear-out failures, aging, and temperature variations. Despite these drawbacks, the constant failure rate method is widely adopted for the reliability evaluation of dc-dc power electronic converters [29-31].

The Markov chain method is implemented here to estimate the lifetime of quadratic buck-boost converters. Markov chain is modeled such that it covers the fully operating condition to complete failure of the power converter. The Markov chain diagram of quadratic buck-boost converters is shown in Fig. 6.

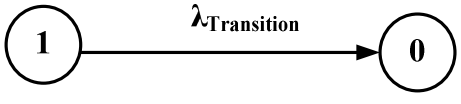

Fig. 6. Markov chain model of the converters T_1 to T_7

TABLE III. COMPONENTS FAILURE RATES

Component	Failure rate models	Temperature factor
MOSFET	$\lambda_S = \lambda_b\,\pi_T\pi_A\pi_Q\pi_E$	$\pi_T = exp\left[-1925\left(\frac{1}{T_j+273}-\frac{1}{298}\right)\right]$
Diode	$\lambda_D = \lambda_b\,\pi_T\pi_S\pi_C\pi_Q\pi_E$	$\pi_T = exp\left[-3091\left(\frac{1}{T_j+273}-\frac{1}{298}\right)\right]$
Inductor	$\lambda_L = \lambda_b\,\pi_T\pi_Q\pi_E$	$\pi_T = exp\left[-\frac{0.11}{8.617\times10^{-5}}\left(\frac{1}{T_j+273}-\frac{1}{298}\right)\right]$
Capacitor	$\lambda_L = \lambda_b\,\pi_{CV}\pi_Q\pi_E$	-

State 1 is the healthy operating condition, where all devices are working correctly. If any device is failed, it will lead to the complete failure of the converter, which is denoted as state 0. $\lambda_{\text{Transition}}$ is the transition rate from the healthy state (state 1) to the failure state (state 0). $\lambda_{\text{Transition}}$ can be computed by adding the failure rates of all the converter components. The probability function Markov model shown in Fig. 6 is given below.

$$\frac{d}{dt}[P_1(t) \quad P_2(t)] = [P_1(t) \quad P_2(t)]\begin{bmatrix}\lambda_{\text{Transition}} & -\lambda_{\text{Transition}}\\ 0 & 0\end{bmatrix} \tag{3}$$

As state 1 is the initial state, the probability of being in state 1 can be computed by considering the initial condition.

$$P(0) = [1\ 0] \tag{4}$$

Substitute the equation (4) in (3) will get the probability for the state 1, and also mean time to failure can be computed by using the relationship given below.

$$\begin{cases} R(t) = P_1(t) = e^{-\lambda_{\text{Transition}}(t)} \\ \text{MTTF} = \int_0^\infty R(t)\,dt = \frac{1}{\lambda_{\text{Transition}}}\ (\times 10^6\ \text{Hours}) \end{cases} \tag{5}$$

To calculate the failure rates of all the components in a power converter, an American military-based handbook MIL-HDBK-217F [32] is used. The failure rate of an electronic component can be calculated by using the below equation.

$$\lambda_{comp} = \lambda_b \prod_{i=1}^{n} \pi_i \tag{6}$$

Where λ_b is the base failure rate of a circuit component (switch/diode/capacitor/inductor); and n is the number of external π factors that affect the component failure rate. The π factors are not the same as all the components; they depend on the corresponding operational and environmental conditions [29]-[31] and are given in Table III. The failure rate of a switch, diode, capacitor, and inductor is denoted with λ_S, λ_D, λ_C, and λ_L, respectively. The Influence π factors of each component are given in Table III. The most significant

TABLE IV. DATASHEET PARAMETERS OF COMPONENTS

MOSFET (IRF 540)	$R_{DS(on)} = 0.07\Omega$, V_T=0.5, C_O= 330 pF, θ_{CA} = 62, θ_{JC} =1, $\lambda_b = 0.06$
Diode (MUR 860)	R_d= 0.07 Ω, V_F=0.5V, θ_{CA} = 73, θ_{JC} =1.5, $\lambda_b = 0.0038$
Inductor	Resr = 0.1 Ω, $\lambda_b = 0.00003$
Capacitor	$\lambda_b = 0.078$

factor is the temperature factor (π_T), it plays a significant role in the failure rate of components like switches and capacitors. The temperature factor is a function of power losses that occur in a particular component and ambient temperature. A detailed explanation about calculating these influence factors is given in [29-31]. These factors can be selected by using the "MIL-HDBK-217F" handbook. The details of device parameters used in this work are given in Table IV.

The same type of components is used to have fair comparison and assumed that all converters have functioned in the same operational and environmental conditions. The calculated failure rate of each converters component, the total failure rate of the system (sum of the failure rates for each element in a converter), and mean time to failure time is given in Table V. The transition failure rate computed with the details as mentioned earlier. Then, the reliability and mean time to failure (MTTF) are estimated using the equation (5). The corresponding reliability curve is drawn with respect to operating time and is shown in Fig. 7. The steepest curve represents the less reliable system. The calculated value of MTTF is given in Table V. From the Fig. 7, it is clear that the topology T_6 has less reliability compared other converters, and fourth-order converters has almost same reliability. Same conclusions can be drawn from MTTF from Table V. The T_6 has very less MTTF value and T_2 has highest MTTF value compared to remaining converters. Over all, the Topology T_7 is shown superiority in terms of less electric stress, SDP, good efficiency, reliability, and low cost.

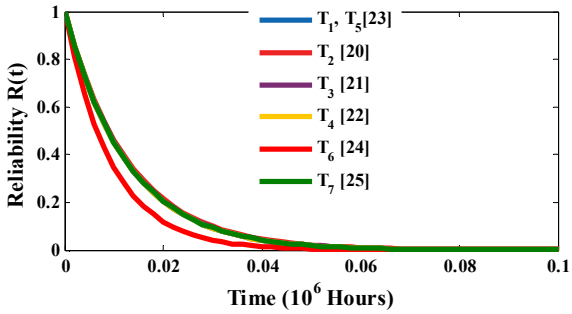

Fig. 7. Reliability comparison of all the converters.

TABLE V. COMPONENT'S FAILURE RATES FOR ALL CONVERTERS

Topology	λ_{S1}	λ_{S2}	λ_{D1}	λ_{D2}	λ_{D3}	λ_{D4}	λ_{D5}	λ_C	λ_L	$\lambda_{\text{Transition}}$	MTTF (10^6 Hours)	Cost
T_1	72.79	5.61	0.15	0.011	-	-	-			79.5335	12600	Low
T_2	70.5	5.5	0.142	0.011	-	-	-			77.1255	13000	Low
T_3	73.28	5.86	0.145	0.015	-	-	-			80.2655	12500	Low
T_4	72.02	5.8	0.14	0.013	-	-	-			78.9455	12700	Low
T_5	72.8	5.7	0.142	0.01	-	-	-			79.6245	12600	Low
T_6	104.8		0.152	0.152	0.014	0.005	0.005	0.486	0.00024	106.1	09400	High
T_7	72.15	5.8	0.15	0.013	-	-	-			79.08	12600	Medium

CONCLUSION

This article evaluates quadratic buck-boost gain converters' performance and compares them for quick selection of a topology suitable for renewable energy applications. Since the gain of all these converters is same, the comparison is made in terms of structural differences, electric stress experienced by the power semiconducting devices, total voltage stress (TVS), total current stress (TCS), and the switch device power rating (SDP). From the electric stress point of view, the topology T_6 experience high TVS, TCS, because of that SDP of T_6 is very high compared to other converters. In addition, the Markov chain model-based reliability analysis is carried out for all the converter. The T_6 has less reliability than other converters. It can be concluded that, the topology T_7 has shown great promise for compare to other converters in terms wide conversion ratio, continuous input and output currents, positive output, common ground, good efficiency and reliability, and minimum phase system.

REFERENCES

[1] M. B. Ferrera Prieto, S. P. Litran, E. D. Aranda and J. M. E. Gomez, "New Single-Input, Multiple-Output Converter Topologies: Combining Single-Switch Nonisolated dc-dc Converters for Single-Input, Multiple-Output Applications," in IEEE Industrial Electronics Magazine, vol. 10, no. 2, pp. 6-20, June 2016.

[2] T.M. Undeland WR, Mohan N, Power electronics converters, applications and design, John Wiley and Sons, New York, 2003

[3] M. Forouzesh, Y. P. Siwakoti, S. A. Gorji, F. Blaabjerg and B. Lehman, "Step-Up DC–DC Converters: A Comprehensive Review of Voltage-Boosting Techniques, Topologies, and Applications," in IEEE Transactions on Power Electronics, vol. 32, no. 12, pp. 9143-9178, Dec. 2017.

[4] M. A. Salvador, J. M. de Andrade, T. B. Lazzarin and R. F. Coelho, "Non-isolated High-Step-Up DC–DC Converter Derived from Switched-Inductors and Switched-Capacitors," in IEEE Transactions on Industrial Electronics, vol. 67, no. 10, pp. 8506-8516, Oct. 2020.

[5] Y. Wang, Y. Qiu, Q. Bian, Y. Guan and D. Xu, "A Single Switch Quadratic Boost High Step Up DC–DC Converter," in IEEE Transactions on Industrial Electronics, vol. 66, no. 6, pp. 4387-4397, June 2019.

[6] S. Naresh and S. Peddapati, "Comparative Analysis of Voltage Multiplier Cell Based Non-Isolated Step-Up Converters," 2020 IEEE International Conference on Power Electronics, Drives and Energy Systems (PEDES), 2020, pp. 1-6.

[7] SVK Naresh, S. Peddapati and V. S. P. K, "Comparison of Double Gain Continuous Input Non-Isolated Boost Converters," 2020 IEEE Students Conference on Engineering Systems (SCES), 2020, pp.1-6.

[8] H. Ardi, A. Ajami and M. Sabahi, "A Novel High Step-Up DC–DC Converter With Continuous Input Current Integrating Coupled Inductor for Renewable Energy Applications," in IEEE Transactions on Industrial Electronics, vol. 65, no. 2, pp. 1306-1315, Feb. 2018.

[9] S. Lee and H. Do, "High Step-Up Coupled-Inductor Cascade Boost DC–DC Converter With Lossless Passive Snubber," in IEEE Transactions on Industrial Electronics, vol. 65, no. 10, pp. 7753-7761, Oct. 2018.

[10] A. R. N. Akhormeh, K. Abbaszadeh, M. Moradzadeh and A. Shahirinia, "High-Gain Bidirectional Quadratic DC–DC Converter Based on Coupled Inductor With Current Ripple Reduction Capability," in IEEE Transactions on Industrial Electronics, vol. 68, no. 9, pp. 7826-7837, Sept. 2021.

[11] R. Tymerski and V. Vorperian, "Generation, Classification and Analysis of Switched-Mode DC-to-DC Converters by the Use of Converter Cells," INTELEC '86 - International Telecommunications Energy Conference, Toronto, Canada, 1986, pp. 181-195.

[12] D. Maksimovic and S. Cuk, "Switching converters with wide DC conversion range," in IEEE Transactions on Power Electronics, vol. 6, no. 1, pp. 151-157, Jan. 1991.

[13] J. A. Morales-Saldana, E. E. C. Gutierrez and J. Leyva-Ramos, "Modeling of switch-mode dc-dc cascade converters," in IEEE Transactions on Aerospace and Electronic Systems, vol. 38, no. 1, pp. 295-299, Jan. 2002.

[14] A. Naderi and K. Abbaszadeh, "High step-up DC–DC converter with input current ripple cancellation," in IET Power Electronics, vol. 9, no. 12, pp. 2394-2403, 5 10 2016, doi: 10.1049/iet-pel.2015.0723.

[15] R. Loera-Palomo and J. A. Morales-Saldaña, "Family of quadratic step-up dc–dc converters based on non-cascading structures," in IET Power Electronics, vol. 8, no. 5, pp. 793-801, 5 2015.

[16] O. Lopez-Santos, J. C. Mayo-Maldonado, J. C. Rosas-Caro, J. E. Valdez-Resendiz, D. A. Zambrano-Prada and O. F. Ruiz-Martinez, "Quadratic boost converter with low-output-voltage ripple," in IET Power Electronics, vol. 13, no. 8, pp. 1605-1612, 2020.

[17] Naresh SVK, Peddapati S. Complementary switching enabled cascaded boost-buck-boost (BS-BB) and buck-boost-buck (BB-BU) converters. Int J Circ Theor Appl, vol. 49, no. 9, pp. 2736-2753, Sep 2021.

[18] Naresh SVK, Peddapati S. New family of transformer-less quadratic buck-boost converters with wide conversion ratio. Int Trans Electr Energ Syst., 1-21, 2021;e13061. doi:10.1002/2050-7038.13061.

[19] Z. Chen, P. Yang, G. Zhou, J. Xu and Z. Chen, "Variable Duty Cycle Control for Quadratic Boost PFC Converter," in IEEE Transactions on Industrial Electronics, vol. 63, no. 7, pp. 4222-4232, July 2016.

[20] S. Miao, F. Wang and X. Ma, "A New Transformerless Buck–Boost Converter With Positive Output Voltage," in IEEE Transactions on Industrial Electronics, vol. 63, no. 5, pp. 2965-2975, May 2016.

[21] A. Mostaan, S. A. Gorji, M. Soltani and M. Ektesabi, "A novel quadratic buck-boost DC-DC converter without floating gate-driver," 2016 IEEE 2nd Annual Southern Power Electronics Conference (SPEC), 2016, pp. 1-5.

[22] Julio C. Rosas-Caro, Victor M. Sanchez, Jesus E. Valdez-Resendiz, Jonathan C. Mayo-Maldonado, Francisco Beltran-Carbajal, Antonio Valderrabano-Gonzalez, Quadratic buck–boost converter with positive output voltage and continuous input current for PEMFC systems,International Journal of Hydrogen Energy, Vol. 42, no. 51, 2017, Pages 30400-30406, ISSN 0360-3199.

[23] J. C. Rosas-Caro, J. E. Valdez-Resendiz, J. C. Mayo-Maldonado, A. Alejo-Reyes and A. Valderrabano-Gonzalez, "Quadratic buck–boost converter with positive output voltage and minimum ripple point design," in IET Power Electronics, vol. 11, no. 7, pp. 1306-1313, 2018.

[24] N. Zhang, G. Zhang, K. W. See and B. Zhang, "A Single-Switch Quadratic Buck–Boost Converter With Continuous Input Port Current and Continuous Output Port Current," in IEEE Transactions on Power Electronics, vol. 33, no. 5, pp. 4157-4166, May 2018.

[25] V. C. Mummadi and M. R. Khuntia, "Design and Analysis of Two-switch Based Enhanced Gain Buck-Boost Converters," in IEEE Transactions on Industrial Electronics, doi: 10.1109/TIE.2021.3071696.

[26] S. Yang, A. Bryant, P. Mawby, D. Xiang, L. Ran and P. Tavner, "An Industry-Based Survey of Reliability in Power Electronic Converters," in IEEE Transactions on Industry Applications, vol. 47, no. 3, pp. 1441-1451, May-June 2011.

[27] Y. Song and B. Wang, "Survey on Reliability of Power Electronic Systems," in IEEE Transactions on Power Electronics, vol. 28, no. 1, pp. 591-604, Jan. 2013.

[28] Tsai-Fu Wu and Yu-Kai Chen, "A systematic and unified approach to modeling PWM DC/DC converters based on the graft scheme," in IEEE Transactions on Industrial Electronics, vol. 45, no. 1, pp. 88-98, Feb. 1998.

[29] E. Jamshidpour, P. Poure and S. Saadate, "Photovoltaic Systems Reliability Improvement by Real-Time FPGA-Based Switch Failure Diagnosis and Fault-Tolerant DC–DC Converter," in IEEE Transactions on Industrial Electronics, vol. 62, no. 11, pp. 7247-7255, Nov. 2015.

[30] P. Zhang, Y. Wang, W. Xiao and W. Li, "Reliability Evaluation of Grid-Connected Photovoltaic Power Systems," in IEEE Transactions on Sustainable Energy, vol. 3, no. 3, pp. 379-389, July 2012.

[31] A. Khosroshahi, M. Abapour and M. Sabahi, "Reliability Evaluation of Conventional and Interleaved DC–DC Boost Converters," in IEEE Transactions on Power Electronics, vol. 30, no. 10, pp. 5821-5828, Oct.2015.

[32] "Reliability prediction of electronic equipment," Department of Defence, Washington DC, Tech. Rep. MIL-HDBK-217F, Dec. 1991.